19th Australasian Fluid Mechanics Conference
Melbourne, Australia
8-11 December 2014

Fouling of Waste Heat Recovery: Numerical and Experimental Results

E. Sauret[1], I. Abdi[2] and K. Hooman[2]

[1]School of Chemistry, Physics & Mechanical Engineering
Queensland University of Technology, Brisbane, Qld 4000, Australia

[2]School of Mechanical & Mining Engineering
The University of Queensland, St Lucia, Qld 4072, Australia

Abstract

Numerical results are presented to investigate the performance of a partly-filled porous heat exchanger for waste heat recovery units. A parametric study was conducted to investigate the effects of inlet velocity and porous block height on the pressure drop of the heat exchanger. The focus of this work is on modelling the interface of a porous and non-porous region. As such, numerical simulation of the problem is conducted along with hot-wire measurements to better understand the physics of the problem. Results from the two sources are then compared to existing theoretical predictions available in the literature which are unable to predict the existence of two separation regions before and after the porous block. More interestingly, a non-uniform interface velocity was observed along the streamwise direction based on both numerical and experimental data.

Introduction

Porous heat exchangers are receiving considerable attention as their application can lead to high heat transfer rates usually associated with a limited footprint. This can be of significant importance in engineering applications such as air-cooled condensers wherein heat exchanger size determines the fan or the cooling tower size. Like other surface extension approaches, however, this heat transfer augmentation technique causes extra pressure drop. Thus it is crucial to minimize the total pressure drop while keeping the augmented heat transfer rate. In order to improve the heat transfer thanks to a surface area increase, fins are added to the tube-bundle heat exchangers. New developments led to further improve the efficiency of heat exchangers by replacing the fins by metal foams [4]. Recently, porous heat exchangers, like metal foams, were suggested as alternatives to fins [5, 6, 8, 14]. It appears that despite the efforts made in the literature, such porous heat exchangers are not well understood and therefore not yet optimized for engineering applications such as heat exchangers. Porous heat exchangers are currently designed using the same knowledge gathered for fins over the years. This, however, is not the best analogy. Recent experimental results, for instance, showed that the wake behind a porous-covered pipe is completely different from those of bare and finned tubes in cross flow [12] and the flow structures are detaching from the wake [1]. This is to be expected as fins act like narrow channels to guide the gas flow in the preferred direction(s). While similar to fins in leading to boundary layer interruption, porous covers lead to a random flow distribution within the pores with different local heat transfer patterns and wall heat flux split [11]. In addition, with any partial blockage of the flow area, another unknown is the problem of the interface modeling between a porous and non-porous region. As recently underlined by Nield and Kuznetsov [15], this interface modelling remains an open question in the literature. While physically one expects much lower fluid velocity in the pores compared to that of free flow, capturing this sharp gradient at the interface can add to the difficulties of numerical simulation. Experiments addressing this issue are, surprisingly, rare. Beavers and Joseph [3] were amongst the first to show that sharp gradients at the interface between the porous and fluid regions exist. Their work highlighted the existence of a slip velocity at the interface. From there, authors have established different interface conditions that can be classified into two main types according to Alazmi and Vafai [2]: slip and no-slip boundary conditions. Those authors then establish five main categories for the hydrodynamic interface conditions and four categories for the thermal interface conditions that they critically examined. The different models mostly lead to comparable results except for few specific cases. To show the complexity of the problem, it is interesting to note that all these works were conducted for duct flows where there is no recirculation or wakes which cannot be modeled as internal flows. This paper does not aim at solving the interface problem but it presents a critical comparison of the theoretical analysis and our numerical simulations and experimental data.

Experiments

Set Up

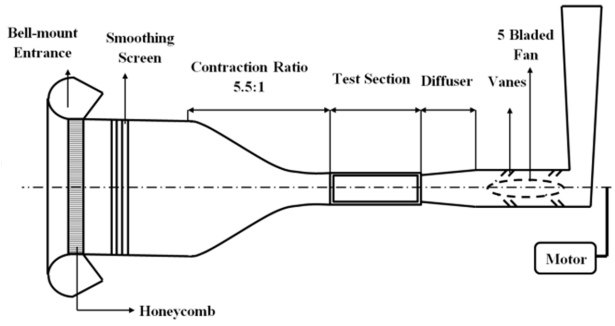

Figure 1. Wind Tunnel Schematic.

Using experimental setup shown in figures 1 and 2, it is possible to observe flow past a block of metal foam at different Reynolds numbers. The experimental setup consists of an open loop suction wind tunnel. Air is drawn into the intake bell- mount by a fan rotor driven by a 17 kW electric motor. The intake consists of a fine mesh screen that is used as a filter to prevent unwanted particles, followed by a honeycomb section containing 1700 cardboard cylinders. Removable flow-smoothing screens are located immediately downstream of these cylinders [10]. The test section of the wind tunnel is a square one. The size of the test section is 300x300x2000 mm3 located in the School of Mechanical and Mining Engineering at the University of Queensland. The test section walls have been constructed out of transparent Plexiglas that allows photography of flow field. The air velocity at the test section inlet is measured by means of a 55P05 Dantec hotwire probe. In figure 1 the stream-wise and the transverse directions are indicated by x and y axes, respectively.

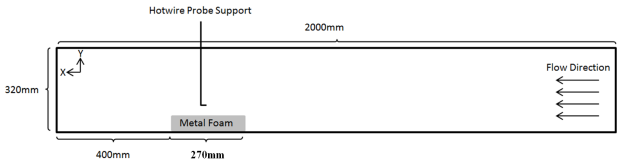

Figure 2. Wind Tunnel Schematic.

All the measurements are made at three different inlet velocities (U) of 3, 6 and 12 m/s. The free stream turbulence level of empty test section was measured as 0.5% at the lowest velocity.

Hotwire Anemometry

In hot-wire measurements, a Dantec 55P15 single sensor hot-wire probe was used. The probe has 1.25 mm long platinum-plated tungsten wire sensing elements of 5μm diameter and is operated in constant temperature mode with an over-heat ratio set to 1.8. The probe was calibrated in the free stream using Dantec 54T29 reference velocity probe. The probe was mounted to a computer controlled three-axis traverse system. Streamwise velocity fluctuations were acquired at linearly spaced cross-section in X downstream of the cylinder with a resolution of 10μm, with sufficient sampling frequency of 10 kHz to resolve the smallest scales and sufficiently long sample lengths for statistical convergence (120 seconds at each point). The uncertainty relative to the maximum velocity at 95% confidence is 1.3%.

Samples

Three metal foam samples with different heights (10, 20 and 50mm) were used to conduct this experiment. The foams are made of an open cell aluminum foam sheet, bonded to a stainless steel plate with dimensions 320 x 270 mm (width x length). Foams consist of ligaments forming a network of interconnected cells. The cells are randomly oriented and are mostly homogeneous in size and shape. The foams PPI is 10 and the effective density varies from 3% to 5% of a solid of the same material.

Numerical Modelling

Computational Domain

The 2D computational domain is presented in figure 3 with a total length L=2m, a total height H_t=0.5m. The foam colored in blue is 0.27m long (L_f). Two foam heights have been experimentally and numerically investigated, H_f=0.02 and 0.05m. In the computational domain, the foam is placed in the middle of the domain so sufficient length before and after the foam are introduced to correctly model the flow.

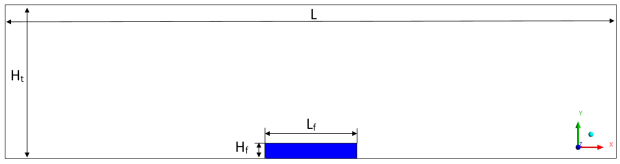

Figure 3. Computational domain.

The characteristics of the foam are given in table **??**.

Grid and Boundary Conditions

The two-dimensional computational grid has 144,672 nodes and a zoom around the foam is presented in figure 4. The grid has been refined at the interface between the porous and non-porous regions. At the walls, a 5-layer inflation was defined with a growth rate of 1.2 with the non-dimensional distance at the wall y_w^+ limited to 5. The convergence of the results was carefully checked and all the residuals dropped below 10^{-6}.

Variables	
K [m^2]	5.3×10^{-7}
ε [-]	0.913
PPI	10
H_f [m]	0.02, 0.05
L_f [m]	0.27

Table 1. Metal Foam Characteristics.

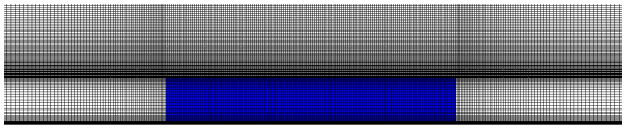

Figure 4. Computational grid in and around the foam.

Numerical Modelling

The 2D simulations were carried out using commercially-available software *Ansys-CFX*. The standard k-ε turbulence model was used for the non-porous region following the work of Odabaee et al. [16].
The metal foam domain has been modelled as an isotropic homogeneous porous media. In the isotropic porous domain, the momentum loss included in the momentum source for the axial direction is expressed using the Hazen-Dupuit-Darcy law (equation 1) as a function of the permeability and the loss coefficients.

$$S_{M,x} = -\frac{dP}{dx} = \frac{\mu_{eff}}{K} u_x + c_F \frac{\rho}{\sqrt{K}} |U| u_x \qquad (1)$$

where c_F=0.1 for 10PPI as given by the experiments, μ_{eff} is the effective viscosity of the porous media. As mentioned by Givler and Altobelli [9] and later by Phanikumar and Mahajan [17], the effective viscosity is not yet well-established in the literature. In this study, the effective viscosity is equal to the main fluid flow viscosity ($\mu_{eff} = \mu_f = 1.831 \times 10^{-5}$ kg.m^{-1}.s^{-1}) as suggested by Phanikumar and Mahajan [17]. At the interface between the porous domain and the main flow, the continuity in shear stress is applied, similarly to the work presented by Ejlali et al. [7].

Results

Comparisons CFD-Experiments

The comparison between the experiments and the numerical results is presented in figure 5 for the 20-mm foam height. The trends of the velocity along the interface are properly reproduced by the numerical model. At the inlet of the foam, the velocity is underestimated by the CFD as the inlet velocity increases. Near the end of the foam, the velocity is slightly underpredicted at all the inlet velocity values.

The velocity profiles for the 2 foam heights 20mm and 50mm are compared in figure 6. While the velocity tends to increase after the intial drop from x=75mm for the 20-mm foam, the velocity continues to decrease for the 50-mm foam. Recirculation is even obtained at $U_\infty = 12m.s^{-1}$.

The non-dimensional velocity profiles at different locations along the foam are plotted in figure 7. The numerical simu-

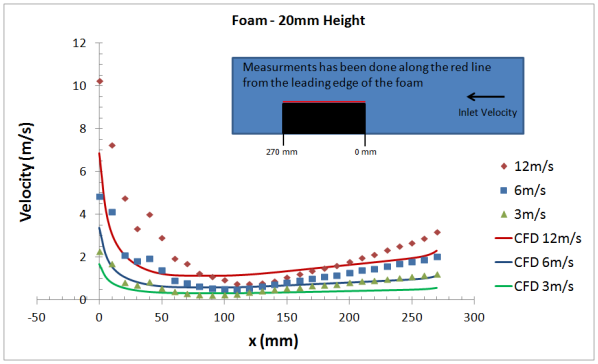

Figure 5. Comparisons of the experimental and numerical velocity profiles at different inlet velocities along the interface for the 20mm-foam height.

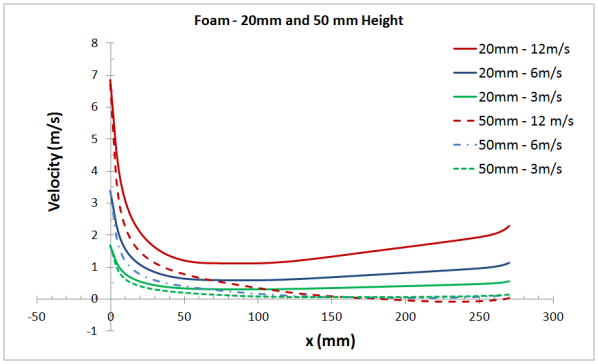

Figure 6. Comparisons of the numerical velocity profiles at different inlet velocities along the interface for the 20mm and 50mm foam heights.

lations are in fairly good agreement with the experimental data. We can also clearly note the separationn of the flow in the foam. For the 20-mm foam the separation ends before reaching the end of the foam while for the 50-mm foam, the separation lasts until the end of the foam and even after as seen in figure 8. For both foams, the effect of the inlet velocity on the separation inside the foam is not significant. However, the separation region is extended after the foam where the velocity increases, especially for the 50-mm foam as shown in figure 8. The height of the foam has also a strong effect on the maximum velocity reached outside the foam. Indeed, in figure 8, we can clearly note the increased region of high speed above the foam for the 50-mm foam as the non-porous flow region decreases with the increase of the foam height. The foam acts as a step for the flow.

Comparisons CFD-Kuznetsov Analytical Profiles

Figure 9 shows a comparison between theoretical results of Kuznetsov [13] and current predictions. Kuznetsov [13] assumes a velocity jump at the interface and predicts a uniform velocity at the interface which does not change along the longitudinal direction. This, however, is not the case according to both numerical predictions and experimental data collected using hot wire anemometry. As seen, the interface velocity is very high when the fluid first gets into the porous medium. This is mainly because a significant part of the flow tries to avoid the porous block. The interface velocity then sharply drops along the flow path. Almost half way through, the interface velocity starts to recover but only slightly. This could be because of a weak flow out of the porous block due to local pressure differences between the air flowing in and outside the porous block. This phenomenon, nonetheless, is not observed nor accounted for in the theoretical models developed by Beavers and Joseph [3] and later applied by some authors including Kuznetsov [13] and de

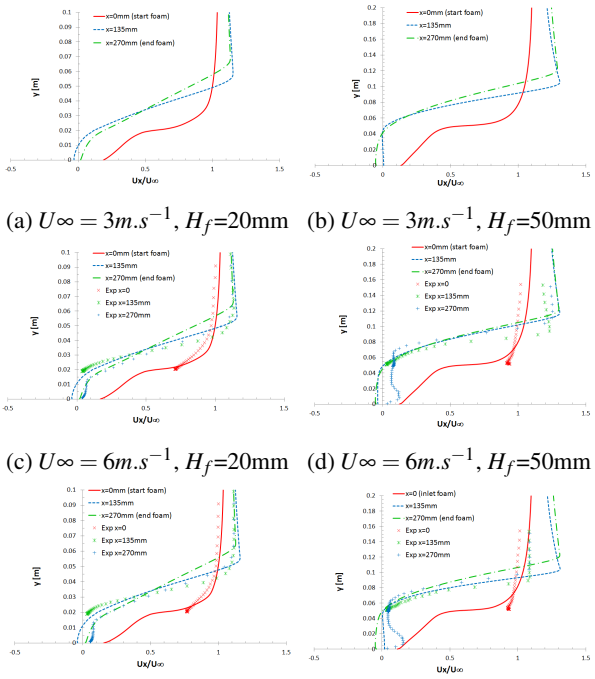

(a) $U\infty = 3m.s^{-1}$, H_f=20mm (b) $U\infty = 3m.s^{-1}$, H_f=50mm

(c) $U\infty = 6m.s^{-1}$, H_f=20mm (d) $U\infty = 6m.s^{-1}$, H_f=50mm

(e) $U\infty = 12m.s^{-1}$, H_f=20mm (f) $U\infty = 12m.s^{-1}$, H_f=50mm

Figure 7. Experimental and numerical non-dimensional axial velocity profiles at different locations along the foam for H_f=20mm and 50mm at the 3 inlet velocities: 3, 6 and $12m.s^{-1}$.

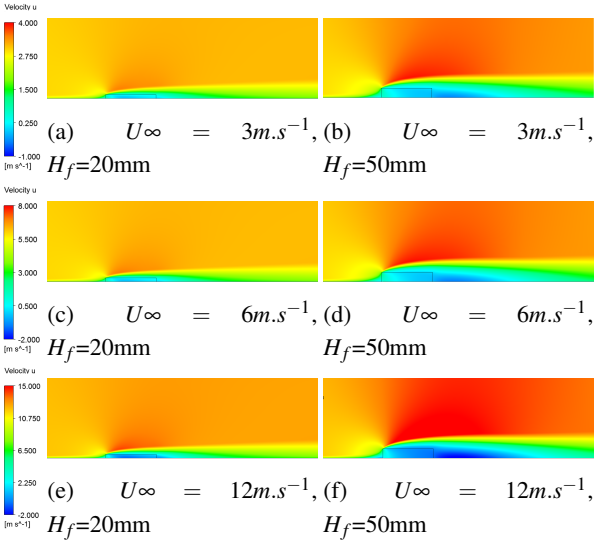

(a) $U\infty = 3m.s^{-1}$, H_f=20mm (b) $U\infty = 3m.s^{-1}$, H_f=50mm

(c) $U\infty = 6m.s^{-1}$, H_f=20mm (d) $U\infty = 6m.s^{-1}$, H_f=50mm

(e) $U\infty = 12m.s^{-1}$, H_f=20mm (f) $U\infty = 12m.s^{-1}$, H_f=50mm

Figure 8. Axial velocity for H_f=20mm (Left) and 50mm (Right) at the 3 inlet velocities: 3, 6 and $12m.s^{-1}$.

Lemos [18]. As a result of a constant and uniform interface velocity, Kuznetsov's velocity profile remains the same in the porous block. However, comparing the inlet and outlet velocity profiles from our CFD simulation, one notes a difference in the profile shapes. This asks for a more detailed simulation and experiment looking into the pore velocity distribution close to the interface. We leave this, however, for a future report.

Conclusions

Hot wire measurements are conducted along with numerical simulation of flow through a partly-porous heat exchanger for waste heat recovery applications. The main goal is to improve

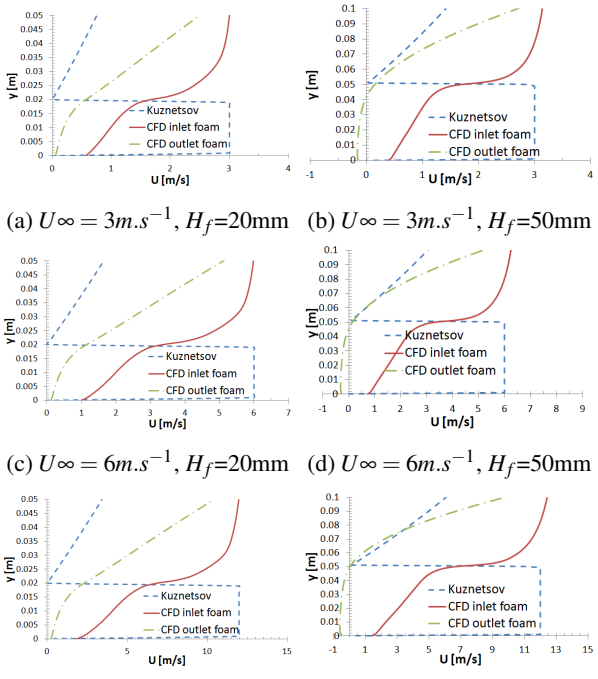

(a) $U\infty = 3m.s^{-1}$, H_f=20mm (b) $U\infty = 3m.s^{-1}$, H_f=50mm

(c) $U\infty = 6m.s^{-1}$, H_f=20mm (d) $U\infty = 6m.s^{-1}$, H_f=50mm

(e) $U\infty = 12m.s^{-1}$, H_f=20mm (f) $U\infty = 12m.s^{-1}$, H_f=50mm

Figure 9. Comparison of the CFD velocity profiles at the inlet and outlet of the foam and the Kuznetsov profile for H_f=20mm and 50mm at the 3 inlet velocities: 3, 6 and $12m.s^{-1}$.

our understanding of the interface of a porous and non-porous region. While numerical results are showing closer agreement to experimental data, theoretical results, obtained based on a velocity jump boundary condition, are found to be inaccurate asking for more detailed analysis of the problem. Two separation regions before and after the porous block were observed. Furthermore, a non-uniform interface velocity was observed along the streamwise direction based on collected experimental data. None of these, separation and non-uniform interface velocity, could have been predicted using theoretical models. Further development of interface models using the data collected here is then left for a future study.

Acknowledgements

References

[1] Abdi, I., Khashehchi, M. and Hooman, K., A comparison between the separated flow structures near the wake of a bare and a foam-covered circular cylinder, in *ASME 2013 Fluids Engineering Division Summer Meeting*, 2013.

[2] Alazmi, B. and Vafai, K., Analysis of fluid flow and heat transfer interfacial conditions between a porous medium and a fluid layer, *International Journal of Heat and Mass Transfer*, **44**, 2001, 1735–1749.

[3] Beavers, G. and Joseph, D., Boundary conditions at a naturally permeable wall, *Journal of Fluid Mechanics*, **30**, 1967, 197–207.

[4] Boomsma, K., Poulikakos, D. and F., Z., Metal foams as compact high performance heat exchangers, *Mechanics of MAterials*, **35**, 2003, 1161–1176.

[5] Calmidi, V. and Mahajan, R., Forced convection in high porosity metal foams, *Journal of Heat Transfer*, **122**, 2000, 557–565.

[6] Cavallini, A., Mancin, S. and Rossetto, L. amd Zilio, C., Air flow in aluminum foam: Heat transfer and pressure drops measurements, *Experimental Heat Transfer*, **23 (1)**, 2010, 94–105.

[7] Ejlali, A., Mee, D., Hooman, K. and Beamish, B., Numerical modelling of the self-heating process of a wet porous medium, *International Journal of Heat and Mass Transfer*, **54**, 2011, 5200–5206.

[8] Garrity, P. T., Klausner, J. F. and Mei, R., Performance of aluminum and carbon foams for air side heat transfer augmentation,, *Journal of Heat*, **132 (12)**, 2010, 121901.

[9] Givler, R. and Altobelli, S., A determination of the effective viscosity for the brinkman-forchheimer flow model, *Journal of Fluid Mechanics*, **258**, 1994, 355–370.

[10] Godden, P., *Base Pressure Measurements for a Turbine Blade with Span-Wise Trailing Edgecoolant Ejection*, Ph.D. thesis, School of Mechanical and Mining Engineering, The University of Queensland, 2001.

[11] Imani, G., Maerefat, M. and Hooman, K., Pore-scale numerical experiment on the effect of the pertinent parameters on heat flux splitting at the boundary of a porous medium, *Transport in Porous Media*, **98 (3)**, 2013, 631–649.

[12] Khashehchi, M., Abdi, I., Hooman, K. and Roesgen, T., comparison between the wake behind finned and foamed circular cylinders in cross-flow, *Experimental Thermal and Fluid Science*, **52**, 2014, 328–338.

[13] Kuznetsov, A., *Handbook of Porous Media - Chapter 6: Analytical Studies of Frorced Convection in Partly Porous Configurations*, CRC Press, Edited by Kambiz Vafai and Hamid A . Hadim, 2000.

[14] Mahjoob, S. and Vafai, K., A synthetis of fluid and thermal transport models for metal foam heat exchangers, *International Journal of Heat and Mass Transfer*, **51**, 2008, 3701–3711.

[15] Nield, D. A. and Kuznetsov, A. V., An historical and topical note on convection in porous media, *Journal of Heat Transfer*, **135**.

[16] Odabaee, M., Hooman, K. and Gurgenci, H., Metal foam heat exchangers for heat transfer augmentation from a cylinder in cross-flow, *Transport in Porous Media*, **86**, 2011, 911–923.

[17] Phanikumar, M. and Mahajan, R., Non-Darcy natural convection in high porosity metal foams, *International Journal of Heat and Mass Transfer*, **45**, 2002, 3781–3793.

[18] Silva, R. A. and de Lemos, M. J. S., Turbulent flow in a channel occupied by a porous layer considering the stress jump at the interface, *International Journa of Heat and Mass Transfer*, **46**, 2003, 5113?5121.